β-Ga_2O_3 nanowires: Synthesis, characterization, and *p*-channel field-effect transistor

Pai-Chun Chang, Zhiyong Fan, Wei-Yu Tseng, A. Rajagopal, and Jia G. Lu[a)]
Department of Chemical Engineering and Materials Science and Department of Electrical Engineering and Computer Science University of California, Irvine, California 92697

(Received 25 May 2005; accepted 30 September 2005; published online 21 November 2005)

Quasione-dimensional Ga_2O_3 nanowires are synthesized via catalytic chemical vapor deposition method. Their morphology and crystal structure are characterized by electron microscopy and x-ray diffraction techniques, and their optical property is studied by photoluminescence measurement. To develop their future application in nanoelectronic devices, the as-grown Ga_2O_3 nanowires are doped with zinc to increase its carrier concentration and subsequently fabricated into field-effect transistors. Electron transport measurements show that the doped nanowires exhibit *p*-type semiconducting behavior with a significant enhancement of conductivity. © *2005 American Institute of Physics*. [DOI: 10.1063/1.2135867]

Gallium oxide (Ga_2O_3) is a trivalent metal-oxide-semiconductor with a band gap of 4.9 eV. Its remarkable thermal and chemical stability renders it suitable for many promising applications. Ga_2O_3 thin film has been extensively studied and implemented as high temperature oxygen sensor,[1] magnetic tunnel junction,[2] and UV-transparent conductive oxide.[3] In recent years, a low dimensional system has become the rising star that draws enormous attention because of the unique properties resulted from its size confinement and high aspect ratio. Quasione-dimensional structures of Ga_2O_3, such as nanowires and nanobelts,[4–6] have been synthesized and characterized.[7,8] However, the electrical transport study on such system has not yet been reported. With the aim of making practical electronics devices, this letter describes the synthesis method, doping process, field-effect-transistor (FET) fabrication and electrical property characterizations.

Ga_2O_3 nanowires were synthesized by catalytic chemical vapor deposition growth via vapor-liquid-solid mechanism.[9] Pure gallium (Ga) metal was used as the source material. Gold (Au) catalysts initiated the growth of Ga_2O_3 nanowires under oxygen flow (2% mixed with argon) at 920 °C. The as-grown products appeared white and were retrieved for structural and optical characterizations, followed by device fabrication and electrical transport measurements.

A scanning electron microscope (SEM) image of the morphology of the Ga_2O_3 nanowires is shown in Fig. 1(a), inset. The range of the diameter of the as-grown nanowires spans from 20 to 120 nm. X-ray diffraction (Siemens D5000) is used to elucidate the structural property of the Ga_2O_3 nanowires. The diffraction peak positions [Fig. 1(a)] are in excellent agreement with the single phase β-Ga_2O_3 powder diffraction pattern (JCPDS card No. 43-1012). The first and second strongest peaks are labeled at (111) and (002) plane positions, respectively. From the intensity variation in the diffraction pattern, we expect that the as-grown nanowires have different preferable growth directions.[10] High-resolution transmission electron microscope (HRTEM) studies demonstrate the different growth directions. Figure 1(b) shows a nanowire having a diameter around 26 nm. The white rectangular region is enlarged and shown in Fig. 1(c) where the lattice fringes and corresponding selected-area-electron diffraction (SAED) pattern can be clearly seen. SAED illustrates that the crystal growth direction is along [111] with spacing about 2.55 Å and has a 16° angle with respect to the nanowire long axis. Figure 1(d) presents another Ga_2O_3 nanowire of 11 nm diameter with a different growth orientation. Its atomically resolved image [Fig. 1(e)] demonstrates that the stacking direction is along [002] and parallel to the nanowire long axis. The interplanar distance of (002) planes is estimated to be around 2.8 Å. To understand the electronic band structure, photoluminescence (PL) measurements with argon ion (Ar^+) laser second harmonic source ($\lambda = 250$ nm) were performed. PL spectra obtained at different temperatures are shown in Fig. 2. The PL intensity has a minimum at room temperature (300 K), and increases monotonically as the temperature decreases. This is due to the suppression of nonradiative recombinations with diminishing thermal agitation, leading to an enhanced radiative recombination efficiency. Two peak positions can be identified at 414 and 432 nm (corresponding to 2.96 and 2.87 eV).[11–13] The broadband blue-green emission is attributed to the recombination of an electron and a hole originated from donors (due to oxygen vacancies) and acceptors (due to gallium-oxygen vacancy pairs).[14,15] These donor-acceptor pairs can form trapped excitons resulting in the blue-green emission according to the following process: $(V_O, V_{Ga})^{\times} + V_O^{\times} \rightarrow (V_O, V_{Ga})' + V_O^{\bullet} + h\nu$.[16]

Ga_2O_3 is a ceramic material that has formidable insulating property at low temperature. In contrast, it exhibits *n*-type semiconducting properties at high temperature.[17] According to our measurement results, the as-grown Ga_2O_3 nanowires show extremely low current level (below 1 pA) at 30 V bias voltage without any doping treatment at room temperature. To improve its electrical properties and versatility in making electronics devices, *p*-type doping is of paramount importance. In this original work, Zn was incorporated as acceptors by a diffusive doping method to increase the conduction carriers in Ga_2O_3 nanowires. Because of the similar ionic size of Zn and Ga atoms (Zn^{2+}: 0.074 nm, Ga^{3+}: 0.062 nm), Zn is a good candidate for substitutional doping

a)Author to whom correspondence should be addressed; electronic mail: jglu@uci.edu

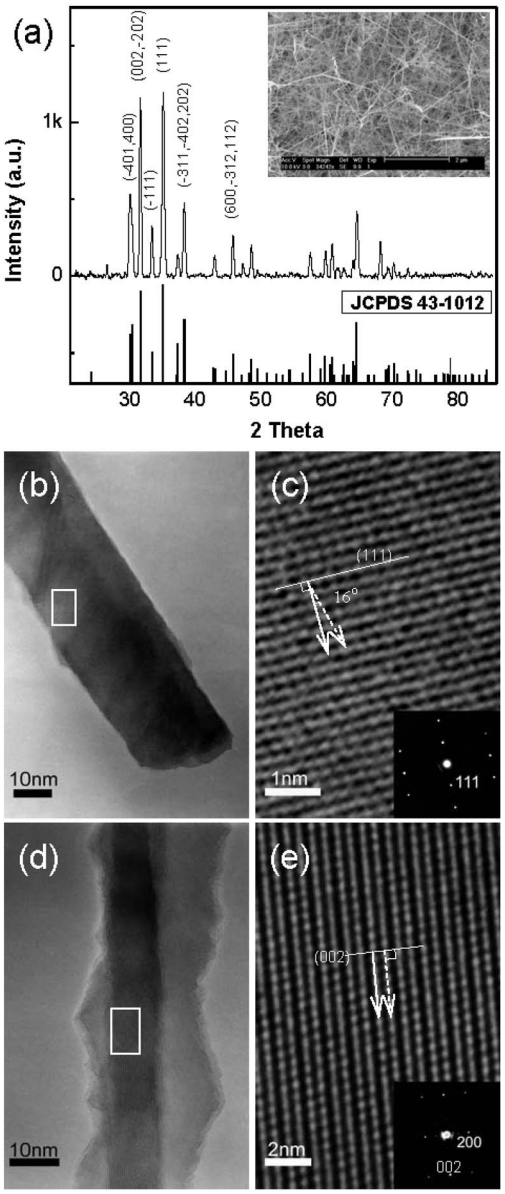

FIG. 1. (a) X-ray diffraction pattern of the as-grown Ga_2O_3 nanowires in comparison to the standard single phase β-Ga_2O_3 from the JCPDS card. The strongest peaks shown are (111) and (002). Inset: SEM image shows the as-grown Ga_2O_3 nanowires distributed on the substrate. The average length is around 20 μm. (b) HRTEM image shows a nanowire having a diameter about 26 nm growing along [111] direction. (c) The distance between the (111) planes is 2.55 Å. The angle between the growth direction (dashed arrow) and the long axis (solid arrow) of the nanowire is approximately 16°. (d) HRTEM image shows another sample with 11 nm diameter growing along [002] direction. (e) Interplanar spacing is about 2.8 Å between the neighboring (002) planes and is about 5.95 Å between (200) planes. The growth direction (dashed arrow) in this case is parallel to the long axis (solid arrow).

governed by $2ZnO \rightarrow 2Zn'_{Ga} + V_O^{\bullet\bullet} + 2O_O$.[1] Ga_2O_3 nanowires and pure Zn powder (99.9% Alfa Aesar) were arranged adjacent to each other in the furnace. The system was first evacuated and then purged with Ar gas to maintain an inert environment. The doping condition was set at 450 °C for the duration of 1 h.

Zn-doped Ga_2O_3 nanowires were then fabricated into FETs for electron transport studies. The nanowires were first dispersed into isopropyl alcohol and then deposited onto p++ silicon chip capped with a 200 nm SiO_2 insulating layer. Photolithography technique was applied to define the

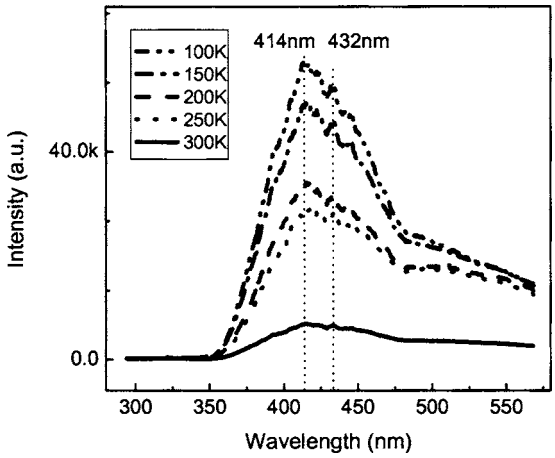

FIG. 2. Photoluminescence spectra show the temperature dependence of intensity. The broadband blue-green emission has two distinguishable peaks, 414 and 432 nm, which correspond to 2.96 and 2.87 eV, respectively.

electrode patterns for attaching metal leads onto individual nanowires. In order to reduce the contact resistance between metal and nanowires, nickel (Ni) has been selected to make p-type FET electrodes due to its large work function. The metallization of the source and drain contacts consists of 20-nm-thick Ni adhesive layer and 300-nm-thick Au lead. A schematic illustration of a nanowire FET configuration is demonstrated in Fig. 3(a), where the p++ silicon layer serves as a backgate. Figure 3(b) is a SEM picture of FET device showing a Ga_2O_3 nanowire channel around 5 μm in length. The Zn-doped Ga_2O_3 nanowire FETs show a large increase in the conductance, with the current level elevated by more than one order of magnitude. I_{ds}-V_{ds} (source-drain current

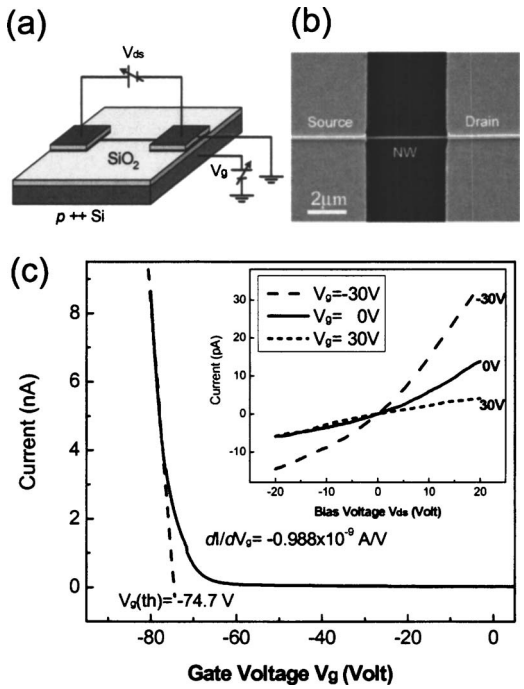

FIG. 3. (a) Schematic view of a nanowire FET configuration. The source and drain contacts are metalized by Ni/Au bilayer, and p++ Si substrate serves as the backgate. (b) SEM picture shows a FET with the nanowire channel about 5 μm in length. (c) $I_{ds}-V_g$ curve at $V_{ds}=20$ V yields transconductance $dI/dV_g=-0.988\times10^{-9}$ A/V and threshold voltage $V_g(\text{th})=-74.7$ V. Inset: $I_{ds}-V_{ds}$ curves under different gate voltages ($V_g=30$, 0, and -30 V) showing p-type semiconducting behavior.

versus bias voltage) behaviors were observed under three different gate voltages (V_g=30, 0, and−30 V) as shown in Fig. 3(c), inset. The results reveal that the current decreases at positive V_g and increases at negative V_g, which manifests *p*-type semiconducting characteristic. This demonstrates that the Zn^{2+} dopants have been substituitionally incorporated into the Ga^{3+} sites in the nanowire lattice, so that the number of the majority carriers (holes) introduced by this doping process exceeds the minority carriers. The extrinsic carrier concentration is proportional to the zinc vapor pressure created inside the doping system.

Furthermore, I_{ds}-V_g (source-drain current versus gate voltage) measurements were performed to analyze the carrier concentration and mobility. The I_{ds}-V_g curve measured from one nanowire FET device [Fig. 3(c)] gives a threshold voltage $V_g(\text{th})=-74.7$ V and a transconductance $dI/dV_g=-0.988\times10^{-9}$ A/V is calculated from the linear region (from $V_g=-75$ to −90 V). From the sample's known parameters, such as the SiO_2 insulating layer h (200 nm), nanowire radius r (60 nm), nanowire channel length L (2.12 μm), and permittivity of SiO_2 ($\varepsilon=3.9$), the quasione-dimensional carrier concentration $p=V_g(\text{th})/e\times2\pi\varepsilon\varepsilon_0/\ln(2h/r)$ and mobility $\mu_h=dI/dV_g\times L\ln(2h/r)/2\pi\varepsilon\varepsilon_0V_{ds}$,[18] can be estimated to be $p=5.3\times10^8$ cm^{-1} and $\mu_h=3.5\times10^{-2}$ cm^2/V s, respectively.

Ga_2O_3 nanowires have been successfully synthesized and characterized. X-ray diffraction spectrum and HRTEM observations show the structural characteristics. In addition, PL measurement is performed to understand the energy band structure. Doping technique has been utilized to enhance the electrical property of Ga_2O_3 nanowire for device applications.[19] In this work, *p*-type Ga_2O_3 nanowires are achieved by using a Zn-doping method. The doped nanowires were fabricated into *p*-channel field-effect transistors for electrical transport studies. Although the as-grown Ga_2O_3 nanowires were found to have structural differences, no significant variation in the transport properties had been observed. The estimated hole mobility ($\sim10^{-2}$ cm^2/V s) is lower than the *p*-type doped GaN nanowires[20] but is comparable to the intrinsic boron nanowires.[21] Our results demonstrate the potential of using Ga_2O_3 nanowire as a building block in future nanoscale devices.

The authors are indebted to Professor Reginald Penner for generous support in PL measurement, to Dr. Wen-An Chiou for HRTEM assistance, and to Dr. Robert Mueller for assistance in low current measurement. Device fabrication was done in Integrated Nanosystems Research Facility (INRF) at the University of California, Irvine. This project is supported by NSF Grant Nos. ECS-0306735 and EEC-0210120.

[1] Y. Li, A. Trinchi, W. Wlodarski, K. Galatsis, and K. Kalantar-Zadeh, Sens. Actuators B **93**, 431 (2003).
[2] Z. Li, C. de Groot, and J. H. Moodera, Appl. Phys. Lett. **77**, 3630 (2000).
[3] H. Ohta, K. Nomura, H. Hiramatsu, K. Ueda, T. Kamiya, H. Hirano, and H. Hosono, Solid-State Electron. **47**, 2261 (2003).
[4] W. Q. Han, P. Kohler-Redlich, F. Ernst, and M. Ruhle, Solid State Commun. **115**, 527 (2000).
[5] Y. C. Choi, W. S. Kim, Y. S. Park, S. M. Lee, D. J. Bae, Y. H. Lee, G. S. Park, W. B. Choi, N. S. Lee, and J. M. Kim, Adv. Mater. (Weinheim, Ger.) **12**, 746 (2000).
[6] H. Z. Zhang, Y. C. Kong, Y. Z. Wang, X. Du, Z. G. Bai, J. J. Wang, D. P. Yu, Y. Ding, Q. L. Hang, and S. Q. Feng, Solid State Commun. **109**, 677 (1999).
[7] C. H. Liang, G. W. Meng, G. Z. Wang, Y. W. Wang, L. D. Zhang, and S. Y. Zhang, Appl. Phys. Lett. **78**, 3202 (2001).
[8] B. Geng, L. Zhang, G. Meng, T. Xie, X. Peng, and Y. Lin, J. Cryst. Growth **259**, 291 (2003).
[9] J. Hu, T. W. Odom, and C. M. Leiber, Acc. Chem. Res. **32**, 435 (1999).
[10] H. J. Chun, Y. S. Choi, S. Y. Bae, H. W. Seo, S. J. Hong, J. Park, and H. Yang, J. Phys. Chem. B **107**, 9042 (2003).
[11] J. Zhang and F. Jiang, Chem. Phys. **289**, 243 (2003).
[12] X. C. Wu, W. H. Song, W. D. Huang, M. H. Pu, B. Zhao, Y. P. Sun, and J. J. Du, Chem. Phys. Lett. **328**, 5 (2000).
[13] J. Zhang, F. Jiang, and L. Zhang, Phys. Lett. A **322**, 362 (2004).
[14] T. Harwing, and F. Kellendouk, J. Solid State Chem. **24**, 255 (1978).
[15] V. I. Yasil'tsiv, Y. M. Zakharko, and Y. I. Prim, Ukr. Fiz. Zh. (Russ. Ed.) **33**, 1320 (1988).
[16] L. Binet and D. Gourier, J. Phys. Chem. Solids **59**, 1241 (1998).
[17] M. Fleischer and H. J. Meixner, Appl. Phys. (N.Y.) **74**, 300 (1993).
[18] R. Martel, T. Schmidt, H. R. Shea, T. Hertel, and P. Avouris, Appl. Phys. Lett. **73**, 2447 (1998).
[19] Y. P. Song, H. Z. Zhang, C. Lin, Y. W. Zhu, G. H. Li, F. H. Yang, and D. P. Yu, Phys. Rev. B **69**, 075304 (2004).
[20] Z. H. Zhong, F. Qian, D. L. Wang, and C. M. Lieber, Nano Lett. **3**, 343 (2003).
[21] D. W. Wang, C. J. Otten, W. E. Buhro, and J. G. Lu, IEEE Trans. Nanotechnol. **3**, 328 (2004).